



**HAL**  
open science

# Unstructured–PEEC Method for Thin Electromagnetic Media

G rard Meunier, Jean-Michel Guichon, Olivier Chadebec, Bertrand Bannwarth, Laurent Kr henb hl, Christophe Gu rin

► **To cite this version:**

G rard Meunier, Jean-Michel Guichon, Olivier Chadebec, Bertrand Bannwarth, Laurent Kr henb hl, et al.. Unstructured–PEEC Method for Thin Electromagnetic Media. IEEE Transactions on Magnet-ics, 2020, 56 (1), 10.1109/TMAG.2019.2951016 . hal-02338778

**HAL Id: hal-02338778**

**<https://hal.science/hal-02338778v1>**

Submitted on 25 Jan 2020

**HAL** is a multi-disciplinary open access archive for the deposit and dissemination of scientific research documents, whether they are published or not. The documents may come from teaching and research institutions in France or abroad, or from public or private research centers.

L'archive ouverte pluridisciplinaire **HAL**, est destin e au d p t et   la diffusion de documents scientifiques de niveau recherche, publi s ou non,  manant des  tablissements d'enseignement et de recherche fran ais ou  trangers, des laboratoires publics ou priv s.

# Unstructured-PEEC Method for Thin Electromagnetic Media

G rard Meunier<sup>1</sup>, Jean-Michel Guichon<sup>1</sup>, Olivier Chadebec<sup>1</sup>, Bertrand Bannwarth<sup>1</sup>,  
Laurent Kr henb hl<sup>2</sup>, Christophe Gu rin<sup>3</sup>

<sup>1</sup>Univ. Grenoble Alpes, CNRS, Grenoble INP, G2Elab, F-38000 Grenoble, France

<sup>2</sup>Univ. Lyon, ECLyon, Amp re, CNRS, France <sup>3</sup>Altair Engineering France, Meylan, France

**Abstract**—An unstructured-PEEC method for modelling electromagnetic thin regions is proposed. Two coupled circuits representations are used for solving both electric and/or magnetic effects in thin regions discretized by a finite element surface mesh. Dynamic effects across the the thickness of the sheet are modeled by equivalent complex conductivity and reluctivity. Non simply connected regions are treated with fundamental branch independent loop matrices coming from the circuit representation. The formulation enables the computation of eddy current losses and can be coupled with external circuits, PEEC cables or coil thanks to the circuit representation.

**Index Terms**—Volume Integral Formulation, Unstructured-PEEC, Thin regions, Losses.

## I. INTRODUCTION

THE electromagnetic modelling of both magnetic and conductive sheets is an important engineering problem frequently encountered in many applications such as the design of shielding devices or planar conductors. The analysis of eddy current distributions is a complex challenge because of the high ratio between the sheet main dimensions and its thickness  $e$  making the volume mesh of the active region very consuming in computing resources with e.g. the finite element method.

Volume Integral Methods (VIM), based on the solving of Maxwell's equations by the volume integration of Green's functions, are very attractive because the air region does not need to be meshed. However, the use of VIM does not prevent from meshing the thickness of the shell in order to catch the high eddy current spatial variation across it due to the skin effect.

Many works have proposed to model the shell with an averaged surface associated to an equivalent electromagnetic behavior for the material. Some formulations, limited to high frequency problems (case  $\delta \ll e$ ), has been presented in [1]-[2]. However, these formulations are limited and do not take into account accurately the skin depth effect at lower frequencies. Very low frequency problems have already been solved but by assuming that the skin depth is high compared to the thickness (case  $\delta \gg e$ ) like in [3]. In [4], the general case is addressed (case  $\delta < e$  or  $\delta \sim e$ ). Equivalent material behavior laws have been proposed in order to represent the field variation across the shell at every frequency. This approach has been used in the context of VIM but limited to the modelling of conductive but non-magnetic materials [5].

Another challenge is the field-circuit coupling which involves a fine mesh of the geometry for local effects while electrical supply and loads are represented by lumped parameters. To use PEEC (Partial Element Equivalent Circuit) method is a good solution. It is a circuit-like integral method which has been applied to shells [6]. The method is very powerful because the circuit representation of the electromagnetic problem makes its coupling with an external electric circuit very easy. However,

the standard PEEC approach is limited to structured meshes and the thickness of the shell has to be meshed in the general case. The PEEC method can be generalized on unstructured mesh as proposed in [7] so it can be applied to every kind of mesh enabling the description of complex geometry. It is based on a volume integral approach based on 3D facet interpolations of the current density and of the magnetic flux density. The approaches can be seen as an unstructured-PEEC method enabling the modelling of both magnetic and conductive regions.

This paper proposes an extension of this unstructured-PEEC method adapted to the modelling of both magnetic and conductive shells in the general case (case  $\delta < e$  or  $\delta \sim e$ ). The equivalent circuit enables coupling with external circuits, PEEC cables or coil. Finally, the use of equivalent properties for modelling dynamic effects along the thickness of the shell ensures the validity of the model in a high range of frequencies and makes the losses computation possible.

## II. FORMULATION

### A. Volume Integral Method

Let us consider a linear frequency-domain magnetic problem with magnetic regions  $\Omega_M$ , conductive region  $\Omega_J$ , and source coils  $\Omega_0$  (with an imposed current density  $\mathbf{J}_0$ ). Based on the solution of Maxwell's equations, electric field  $\mathbf{E}$  and magnetic field  $\mathbf{H}$  can be linked to the current densities  $\mathbf{J}$  and  $\mathbf{J}_0$ , and to the magnetization  $\mathbf{M}$  with integral expression over the conducting  $\Omega_J$  ( $\mathbf{J} \neq 0$ ) and magnetic  $\Omega_M$  ( $\mathbf{M} \neq 0$ ) domains. In the frequency domain, by neglecting capacitive and propagation effects, and thanks to Lorentz gauge, we have:

$$\begin{aligned} \mathbf{E}(P) &= -j\omega\mathbf{A}(P) - \mathbf{grad}V(P) \\ \mathbf{H}(P) &= \mathbf{T}(P) - \mathbf{grad}\varphi(P) \end{aligned} \quad (1)$$

with

$$\begin{aligned} \mathbf{T}(P) &= \frac{1}{4\pi} \left( \iint_{\Omega_J} \mathbf{J} \times \mathbf{grad} \frac{1}{r} d\Omega + \iint_{\Omega_0} \mathbf{J}_0 \times \mathbf{grad} \frac{1}{r} d\Omega \right) \\ \mathbf{A}(P) &= \frac{\mu_0}{4\pi} \left( \iint_{\Omega_J} \frac{\mathbf{J}}{r} d\Omega + \iint_{\Omega_0} \frac{\mathbf{J}_0}{r} d\Omega + \iint_{\Omega_M} \mathbf{M} \wedge \mathbf{grad} \frac{1}{r} d\Omega \right) \\ V(P) &= \frac{1}{j\omega} \frac{1}{4\pi\epsilon_0} \iint_{\Omega_J} \mathbf{J} \cdot \mathbf{grad} \frac{1}{r} d\Omega \\ \varphi(P) &= \frac{1}{4\pi} \iint_{\Omega_M} \mathbf{M} \cdot \mathbf{grad} \frac{1}{r} d\Omega \end{aligned} \quad (2)$$

In these expressions  $r$  is the distance between observation point  $P$  and integration point in media. Volume integral equations are then obtained by matching expression of  $\mathbf{E}$  and  $\mathbf{H}$  with the constitutive relationships  $\mathbf{E}(\mathbf{J})$  and  $\mathbf{H}(\mathbf{M})$  inside the media. Different formulations can be achieved by discretizing

the regions and by choosing adequate unknowns and interpolation basis functions. The use of 2-form Whitney face interpolation associated to both current density  $\mathbf{J}$  and magnetic flux density  $\mathbf{B}$  leads to the unstructured PEEC method [7].

### B. Thin regions model

In the case of thin regions, we consider that the evaluation outside of the media of  $\mathbf{A}$  and  $\mathbf{T}$  in equation (2) can be obtained by using the averaged tangential current and magnetisation  $\mathbf{J}_m$  and  $\mathbf{M}_m$  flowing in the thin regions:

$$\mathbf{A}(P) \approx \frac{\mu_0}{4\pi} \left( \int_{\Gamma_J} e \frac{\mathbf{J}_m}{r} d\Gamma + \iint_{\Omega_0} \frac{\mathbf{J}_0}{r} d\Omega + \int_{\Gamma_M} e \mathbf{M}_m \wedge \mathbf{grad} \frac{1}{r} d\Gamma \right) \quad (3)$$

$$\mathbf{T}(P) \approx \frac{1}{4\pi} \left( \int_{\Gamma_J} e \mathbf{J}_m \wedge \mathbf{grad} \frac{1}{r} d\Gamma + \iint_{\Omega_0} \mathbf{J}_0 \wedge \mathbf{grad} \frac{1}{r} d\Omega \right)$$

where  $e$  is still the thickness of thin regions,  $\Gamma_M$  and  $\Gamma_J$  are the average surface regions of  $\Omega_M$  and  $\Omega_J$ . Equivalent material behavior laws, which take into account dynamic effects across the thickness, can be used. Following [4], these equivalent properties link averaged surface electric and magnetic fields  $\mathbf{E}_{sm}$ ,  $\mathbf{H}_{sm}$  to averaged current and flux densities  $\mathbf{J}_m$ ,  $\mathbf{B}_m$ :

$$\mathbf{E}_{sm} = \frac{\mathbf{J}_m}{G\sigma} \quad \mathbf{H}_{sm} = \frac{\mathbf{B}_m}{G\mu} \quad G = \frac{\tanh\left(\frac{(1+j)e}{\delta}\right)}{(1+j)\frac{e}{\delta}} \quad (4)$$

where  $\sigma$  is the conductivity,  $\mu = \mu_0 \mu_r$  is the permeability and  $\delta$  is the skin depth. Integral equations are then obtained by matching expressions of (1) on the external surfaces of the thin region with constitutive relationships (3). It leads to surface integral equations with  $\mathbf{J}_m$  and  $\mathbf{B}_m$  as unknowns.

### C. Use of 2D face element on 3D surface

The region  $\Gamma$  is discretized by a surface finite element mesh (composed of triangles and/or quadrangles) on which  $\mathbf{J}_m$  and  $\mathbf{B}_m$  are interpolated with 2D first order face elements, i.e. 2D 2-forms:

$$\mathbf{J}_m = \frac{1}{e} \sum_j \mathbf{w}_{sj} I_{sj} \quad \mathbf{B}_m = \frac{1}{e} \sum_j \mathbf{w}_{sj} \phi_{sj}$$

where  $\mathbf{w}_{sj}$  is the face function related to  $j$ -th face,  $I_{sj}$  and  $\phi_{sj}$  are the current (in A) and magnetic flux (in Wb) flowing through the  $j$ -th face, respectively. Let us notice that, with a surface mesh, face elements are associated to the edges of the mesh. We have:

$$\text{div } \mathbf{w}_{si} = \pm \frac{1}{s_e} \quad \mathbf{w}_{si} \cdot \mathbf{n}_i = \pm \frac{1}{l_i} \quad (5)$$

where  $s_e$  is the area of the  $e$ -th element, and  $l_i$  and  $\mathbf{n}_i$  are respectively the length and the normal of  $i$ -th face (geometric edge). The signs in (5) depend on the choice of the global

orientation of the face. These relations ensure the continuity of  $\mathbf{J}_m \cdot \mathbf{n}$  and  $\mathbf{B}_m \cdot \mathbf{n}$  between adjacent elements. By using (5), considering scalar potentials  $V$  and  $\varphi$  and thanks to the divergence theorem, we have (Fig. 1):

$$\int_{\Gamma_J} \mathbf{w}_{is} \cdot \mathbf{grad} V = \Delta V_i \quad \int_{\Gamma_M} \mathbf{w}_{is} \cdot \mathbf{grad} \varphi = \Delta \varphi_i \quad (6)$$

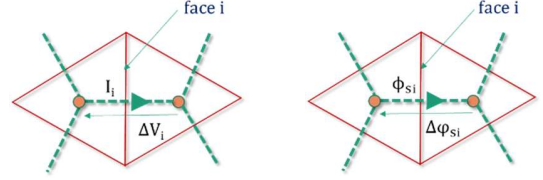


Fig. 1. Primal and dual mesh (dotted lines).  $\Delta V_i$  and  $\Delta \varphi_i$  are the difference between the two mean values of potentials  $V$  and  $\varphi$  in both adjacent elements connected to face  $i$

These properties will be useful to construct an equivalent circuit representation based on the dual mesh, as developed in the next section.

### D. Unstructured PEEC model for thin regions

Applying a Galerkin projection with facet functions  $\mathbf{w}_i$  on equations (1), and by considering (3), (4) and (6), we get a circuit representation on the dual mesh:

$$\begin{cases} \Delta V_s \\ \Delta \varphi_s \end{cases} = \begin{cases} R_s + j\omega L_s & j\omega C_s \\ C'_s & Y \end{cases} \begin{cases} I_s \\ \phi_s \end{cases} + \begin{cases} S \\ T \end{cases} \quad (7)$$

with

$$R_{sij} = \int_{\Gamma_J} \frac{1}{e} \frac{\mathbf{w}_i \mathbf{w}_j}{G\sigma} d\Omega \quad L_{sij} = \frac{\mu_0}{4\pi} \int_{\Gamma_J} \mathbf{w}_i \int_{\Gamma_J} \frac{\mathbf{w}_j}{r} d\Gamma d\Gamma$$

$$Y_{ij} = \int_{\Gamma_M} \frac{1}{e} \frac{\mathbf{w}_i \mathbf{w}_j}{G\mu} d\Omega$$

$$C_{sij} = \frac{1}{4\pi} \int_{\Gamma_J} \mathbf{w}_i \int_{\Gamma_M} \frac{\mu_r - 1}{\mu_r} \mathbf{w}_j \wedge \mathbf{grad} \frac{1}{r} d\Gamma d\Gamma$$

$$C'_{sij} = \frac{1}{4\pi} \int_{\Gamma_M} \mathbf{w}_i \int_{\Gamma_J} \mathbf{w}_j \wedge \mathbf{grad} \frac{1}{r} d\Gamma d\Gamma$$

$$S = \frac{j\omega \mu_0}{4\pi} \int_{\Gamma} \mathbf{w}_{si} \int_{\Omega_0} \frac{\mathbf{J}_0}{r} d\Omega d\Gamma$$

$$T = \frac{1}{4\pi} \int_{\Gamma} \mathbf{w}_{si} \iint_{\Omega_0} \mathbf{J}_0 \wedge \mathbf{grad} \frac{1}{r} d\Omega d\Gamma$$

The equivalent circuit (on the dual mesh) is composed of branches connecting two adjacent elements (i.e. face of the primal mesh), where elements are the nodes of the dual mesh.  $\{\Delta V_s\}$  and  $\{\Delta \varphi_s\}$  represent the differences of electric and magnetic potentials on the branches of the dual mesh.  $R_s$  and  $Y$  are sparse finite element matrices while  $L_s$ ,  $C_s$  and  $C'_s$  are full interaction matrices. Let us notice that  $R_s$  can be physically seen as an equivalent resistance matrix,  $Y$  an equivalent reluctance matrix,  $L_s$  the inductance matrix,  $C_s$  and  $C'_s$  the interaction matrices coupling both conductive and magnetic effects.

In order to take into account magnetic fluxes flowing out from magnetic regions, equations (7) must be completed. The

value of the magnetic potentials on each face element of  $\Gamma_M$  can be obtained from equations (2). Considering a constant permeability for each magnetic region, we have  $\text{div}\mathbf{M}=0$  inside  $\Omega_M$ , and then, using the divergence theorem:

$$\begin{aligned} \iint_{\Omega_M} \mathbf{M} \cdot \mathbf{grad} \frac{1}{r} d\Omega &\approx \int_{\partial\Omega_M} \mathbf{M} \cdot \mathbf{n} d\Gamma \\ &= \frac{1}{\mu_0} \sum_k \int_{\Gamma_{Mk}} \frac{\mu_r - 1}{\mu_r} \frac{1}{s_1} \phi_{ek} d\Gamma \end{aligned}$$

where  $\phi_{ek}$  is the magnetic flux flowing out from both sides of face element  $k$  of the magnetic region.

The averaged value of magnetic potentials on each element of  $\Gamma_M$  can then be written as:

$$\{\varphi_e\} = Q \{\phi_e\}$$

with

$$Q_{kl} = \frac{1}{4\pi\mu_0} \int_{\Gamma_{Mk}} \frac{1}{s_k} \int_{\Gamma_{Ml}} \frac{\mu_r - 1}{\mu_r} \frac{1}{s_1} d\Gamma d\Gamma$$

$\{\phi_e\}$  are the magnetic fluxes flowing out from both external faces elements of  $\Gamma_M$ . By considering that the magnetic potential is null at infinity, the magnetic circuit is completed by adding branches which connect nodes (i.e. surface elements) of  $\Gamma_M$  to the infinity (Fig. 2).

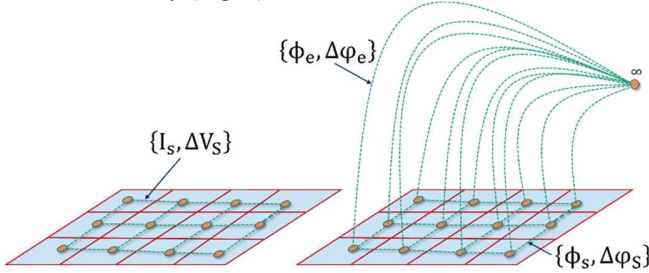


Fig. 2. Example of electric (left) and magnetic (right) equivalent circuits for a plate meshed with quadrangles

Then, the complete set of equations which leads to the equivalent circuit interpretation of the low frequency electromagnetic problem is given by :

$$\begin{Bmatrix} \Delta V_s \\ \Delta \varphi_s \\ \Delta \varphi_e \end{Bmatrix} = \begin{Bmatrix} R_s + j\omega L_s & j\omega C_s & 0 \\ C'_s & Y & 0 \\ 0 & 0 & Q \end{Bmatrix} \begin{Bmatrix} I_s \\ \phi_s \\ \phi_e \end{Bmatrix} + \begin{Bmatrix} S \\ T \\ 0 \end{Bmatrix} \quad (8)$$

The solution can then be obtained using a circuit solver based on an independent loop search technique which provides a unique solution. In practice fundamental circuit equations to be solved are:

$$[M_I] \{\Delta V_s\} = 0$$

$$[M_\phi] \{\Delta \varphi\} = 0 \quad \text{with} \quad \{\Delta \varphi\} = \begin{Bmatrix} \Delta \varphi_s \\ \Delta \varphi_e \end{Bmatrix}$$

where  $[M_I]$  and  $[M_\phi]$  are the branch-fundamental independent loop matrices (also known as incidence matrices) of the electric and magnetic equivalent circuit representations, respectively. The unknowns of the system to be solved are the mesh currents  $I_M$  and mesh flux density  $\phi_M$ :

$$\begin{aligned} \{I\} &= [M_I^t] \{I_M\} \quad \text{with} \quad \{I\} = \{I_s\} \\ \{\phi\} &= [M_\phi^t] \{\phi_M\} \quad \text{with} \quad \{\phi\} = \begin{Bmatrix} \phi_s \\ \phi_e \end{Bmatrix} \end{aligned}$$

The final system to be solved is:

$$\begin{Bmatrix} [M_I][Z_I][M_I^t] & [M_I][Z_{I\phi}][M_\phi^t] \\ [M_\phi][Z_{\phi I}][M_I^t] & [M_\phi][Z_\phi][M_\phi^t] \end{Bmatrix} \begin{Bmatrix} I_M \\ \phi_M \end{Bmatrix} = \begin{Bmatrix} U_I \\ U_\phi \end{Bmatrix} \quad (9)$$

with

$$\begin{aligned} [Z_I] &= [R_s + j\omega L_s] & [Z_{I\phi}] &= [j\omega C_s \quad 0] \\ [Z_{\phi I}] &= \begin{bmatrix} C'_s \\ 0 \end{bmatrix} & [Z_\phi] &= \begin{bmatrix} Y & 0 \\ 0 & Q \end{bmatrix} \\ \{U_I\} &= [M_I] \begin{Bmatrix} S \\ 0 \end{Bmatrix} & \{U_\phi\} &= [M_\phi] \begin{Bmatrix} T \\ 0 \end{Bmatrix} \end{aligned}$$

In the case of conducting regions only, the magnetic unknowns are not needed and the system to be solved becomes:

$$[M_I][Z_I][M_I^t] \{I_M\} = \{U_I\}$$

#### E. Taking into account PEEC cable and circuit coupled coil

In this section, we present the extension of the proposed formulation in order to consider PEEC cable elements and/or coils with circuit coupling (region  $\Omega_c$ ). Each coil and PEEC cable element are characterized by a vector  $\mathbf{j}_{0j}$  such as  $\mathbf{J} = \mathbf{j}_{0j} I_{cj}$ .

The previous system of equations can then be easily adapted by considering the currents  $\{I_c\}$  flowing in these regions. By adapting the system of equations (9), we get:

$$\begin{aligned} \{\phi\} &= \begin{Bmatrix} \phi_s \\ \phi_e \end{Bmatrix} & \{I\} &= \begin{Bmatrix} I_s \\ I_c \end{Bmatrix} \\ [Z_I] &= \begin{bmatrix} R_s + j\omega L_s & j\omega L_{sc} \\ j\omega L_{cs} & R_c + j\omega L_c \end{bmatrix} & [Z_{I\phi}] &= \begin{bmatrix} j\omega C_s & 0 \\ j\omega C_1 & 0 \end{bmatrix} \\ [Z_{\phi I}] &= \begin{bmatrix} C'_s & C'_1 \\ 0 & 0 \end{bmatrix} & [Z_\phi] &= \begin{bmatrix} Y & 0 \\ 0 & Q \end{bmatrix} \end{aligned}$$

with

$$\begin{aligned} R_{cii} &= \int_{\Omega_c} \frac{\mathbf{j}_{0i} \mathbf{j}_{0i}}{\sigma} d\Omega & L_{cij} &= \frac{\mu_0}{4\pi} \int_{\Omega_c} \mathbf{j}_{0i} \int_{\Omega_c} \frac{\mathbf{j}_{0j}}{r} d\Gamma d\Gamma \\ L_{clij} &= \frac{\mu_0}{4\pi} \int_{\Gamma_j} \mathbf{w}_i \int_{\Omega_c} \frac{\mathbf{j}_{0j}}{r} d\Gamma d\Omega \\ L_{lcij} &= \frac{\mu_0}{4\pi} \int_{\Omega_c} \mathbf{j}_{0i} \int_{\Gamma_j} \frac{\mathbf{w}}{r} d\Gamma d\Omega \\ C_{lij} &= \frac{1}{4\pi} \int_{\Omega_c} \mathbf{j}_{0i} \iint_{\Gamma_M} \frac{\mu_r - 1}{\mu_r} \mathbf{w}_j \wedge \mathbf{grad} \frac{1}{r} d\Omega d\Gamma \\ C'_{lij} &= \frac{1}{4\pi} \int_{\Gamma_M} \mathbf{w}_i \int_{\Omega_c} \mathbf{j}_{0j} \wedge \mathbf{grad} \frac{1}{r} d\Gamma d\Omega \end{aligned}$$

Finally, external circuit elements composed of passive components, current or voltage sources can complete the system (9), through electric nodal connections.

#### F. Considerations on implementation

In order to get a good accuracy, the integrations of Green's kernels are computed by using the analytical integration techniques proposed in [8] for self or very close interactions. Moreover, an adaptive mesh integration is used to compute

cable PEEC interaction terms. Let us notice that non-simply connected electric domains are naturally treated thanks to the incidence matrix  $M_I$ . In practice, the circuit solver uses a specific algorithm adapted from [9] with the advantage of favoring small loops. The circuit solver uses a GMRES algorithm combined with an LU decomposition-based preconditioner for sparse matrices R and Y.

### III. RESULTS

We first present an academic problem constituted of a magnetic and conductive thin sphere (diameter 1m, thickness 1mm,  $\mu_r = 1000$ ,  $\sigma = 5 \cdot 10^5$ S/m) placed in a field produced by a cylinder coil, fed by current or voltage source thanks to the coil circuit coupling. The results are compared with a reference solution obtained with an axi-symmetrical FEM using a mesh ensuring the accuracy of the solution at any frequency. Fig. 3 compares eddy current losses obtained with both simulations. In the case of the unstructured-PEEC method, losses are computed by using the equivalent material properties [4]:

$$\text{Losses} = e \int_{\Gamma} \text{Real} \left\{ \frac{\mathbf{J}_m \overline{\mathbf{J}_m}}{G\sigma} - j\omega \frac{\mathbf{B}_m \overline{\mathbf{B}_m}}{G\mu} \right\} d\Gamma \quad (10)$$

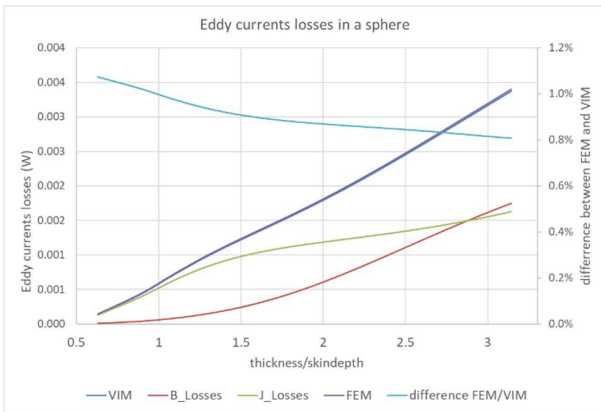


Fig. 3: Losses (W) in a thin sphere. Comparison between unstructured-PEEC VIM and FEM methods for various ratio  $e/\delta$ . The two loss contributions coming from  $B_m$  and  $J_m$  solutions (10) are displayed.

Results obtained are very satisfactory (difference lower than 1% at any frequencies) if we consider the difficulty of accurately calculating eddy current losses.

We also test the formulation on a more complex example dealing with the computation of eddy currents and magnetic flux density in a car body. The magnetic source field is produced by a set of cable fed by a voltage or current source. The surface mesh of the car contains about 18.000 triangles and a HCA matrix compression technique (Hybrid Cross Approximation) still associated to the GMRES linear solver has been used for the solving.

Figure 4 shows the electric loops around holes whereas Fig.5 shows current density and tangential magnetic field on the car body.

### IV. CONCLUSION

The new formulation enables the modeling of thin conductive and/or magnetic regions in order to simulate efficiently various devices with only a surface mesh. The

computational effort is considerably reduced in comparison with volume approaches. Equivalent material properties enable the computation of eddy currents losses with a good accuracy at any frequency. Let us notice that the approach is limited to harmonic problems, an interesting extension could be to consider transient ones.



Fig. 4: Mesh of car body and loops found by the circuit solver to take into account multiply connected electric problems

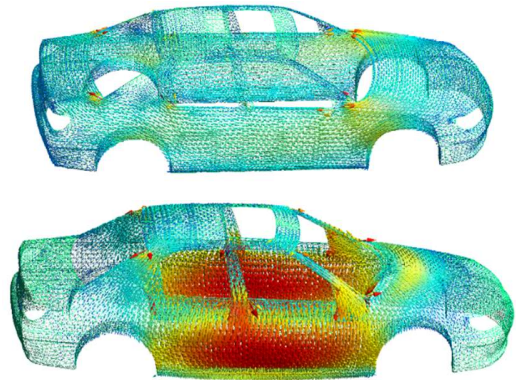


Fig. 5: Example of eddy currents (top) and magnetic flux density (bottom) on a car body

### REFERENCES

- [1] G. Miano and F. Villone, "A surface integral formulation of Maxwell equations for topologically complex conducting domains," *IEEE Trans. Antennas Propag.*, vol. 53, no. 12, pp. 4001-4014, Dec. 2005.
- [2] Z. G. Qian and W. C. Chew, "Fast full-wave surface integral equation solver for multiscale structure modeling," *IEEE Trans. Antennas Propag.*, vol. 57, no. 11, pp. 3594 – 3601, Nov. 2009.
- [3] H-S. Lopez *et al.*, "Multilayer integral method for simulation of eddy currents in thin volumes of arbitrary geometry produced by MRI gradient coils," *Magn. Reson. Med.*, vol. 71, no. 5, pp. 1912-1922, May 2014.
- [4] L. Krähenbühl and D. Müller, "Thin layers in electrical engineering-example of shell models in analysing eddy-currents by boundary and finite element methods," *IEEE Trans. Magn.*, vol. 29, no. 2, pp. 1450-1455, Mar. 1993.
- [5] T. Le-Duc *et al.*, "A new integral formulation for eddy current computation in thin conductive shells," *IEEE Trans. Magn.*, vol. 48, no. 2, pp. 427-430, Feb. 2012.
- [6] D. Gope *et al.*, "(S)PEEC: Time- and frequency- domain surface formulation for modeling conductors and dielectrics in combined circuit electromagnetic simulations," *IEEE Trans. Microw. Theory Tech.*, vol. 54, no. 6, pp. 2453-2464, Jun. 2006.
- [7] G. Meunier, O. Chadebec and J. M. Guichon, "A magnetic flux-electric current volume integral formulation based on facet elements for solving electromagnetic problems," *IEEE Trans. Magn.*, vol. 51, no. 3, Mar. 2015.
- [8] M. Fabbri, "Magnetic flux density and vector potential of uniform polyhedral sources," *IEEE Trans. Magn.*, vol. 44, no. 1, pp. 3236, Jan. 2008.
- [9] J. D. Horton, "A Polynomial-Time Algorithm to Find the Shortest Cycle Basis of a Graph," *SIAM Journal on Computing*, Apr. 1987.